LETTERS

# Gene network shaping of inherent noise spectra

D. W. Austin[1,3], M. S. Allen[1,3], J. M. McCollum[3], R. D. Dar[1], J. R. Wilgus[3], G. S. Sayler[3], N. F. Samatova[2], C. D. Cox[3] & M. L. Simpson[1,3]

**Recent work demonstrates that stochastic fluctuations in molecular populations have consequences for gene regulation[1–10]. Previous experiments focused on noise sources or noise propagation through gene networks by measuring noise magnitudes. However, in theoretical analysis, we showed that noise frequency content is determined by the underlying gene circuits, leading to a mapping between gene circuit structure and the noise frequency range[11,12]. An intriguing prediction from our previous studies was that negative autoregulation shifts noise to higher frequencies where it is more easily filtered out by gene networks[11]—a property that may contribute to the prevalence of autoregulation motifs (for example, found in the regulation of ~40% of *Escherichia coli* genes). Here we measure noise frequency content in growing cultures of *E. coli*, and verify the link between gene circuit structure and noise spectra by demonstrating the negative autoregulation-mediated spectral shift. We further demonstrate that noise spectral measurements provide mechanistic insights into gene regulation, as perturbations of gene circuit parameters are discernible in the measured noise frequency ranges. These results suggest that noise spectral measurements could facilitate the discovery of novel regulatory relationships.**

We investigated single gene circuits on high copy number plasmids (pGFPasv) in *E. coli* TOP10 cells where destabilized (half-life ~110 min) green fluorescent protein (GFP) was constitutively expressed (Fig. 1a). The average GFP fluorescence, which corresponded to the concentration of mature GFP protein, was measured in individual cells in growing cultures for 4–8 h periods using time-lapse microscopy[1,2] (see the Supplementary Movie). Cells remained in the exponential growth phase throughout the experiment. Fluorescence was recorded every 5 min through multiple generations of cell division (Fig. 1b), and noise was found as the difference between the fluorescence of individual cells and the population mean determined at each measurement time (Fig. 1c). Individual noise traces (trajectories) that spanned the entire growth time were constructed by combining sequential noise traces of cells through lines of descent (Fig. 1b and Supplementary Information). Normalized autocorrelation functions of noise in fluorescence were estimated for individual trajectories ($\Phi_m(\tau)$) and composites ($\Phi_c(\tau)$) of all tracked trajectories in each cell culture for the duration of the experiment (Fig. 1d). The composite autocorrelation functions provided the better estimate of the underlying random process, while individual trajectory autocorrelation functions may provide insights into gene circuit structure or function as described below.

Histograms of noise frequency ranges (see Box 1) extracted from the individual trajectory autocorrelation functions (Fig. 2a, b) were compiled and compared with noise frequency range distributions found from exact stochastic simulation[13,14] using a model that included intrinsic and extrinsic noise, protein dilution and protein decay (see the Supplementary Information). The simulations produced as much data as 500 separate experiments, and the resulting distributions estimated the probability of finding a given noise frequency range from a randomly selected trajectory. Experimental distributions were drawn from this random process and were subject to variation, particularly the relatively rare events in the high-frequency tails. Although some measured distributions suggested a bimodal distribution (Fig. 2), this was probably due to non-representative sampling of the rare high-frequency events (see the Supplementary Information).

Analytical models predict that protein dilution and decay rates are dominant factors defining the noise frequency range in constitutively expressed gene circuits[11] (Box 1). To determine noise frequency range sensitivity to protein dilution, we varied cell growth rate for the pGFPasv circuits by controlling temperature, and in a separate experiment we changed the protein decay rate using a plasmid (pGFPaav) containing a reduced half-life (~60 min) GFP variant[15]. These perturbations to gene circuit parameters were clearly visible in the noise spectral measurements, as noise frequency ranges extended to higher frequencies as a result of faster growth (Fig. 2a) or higher

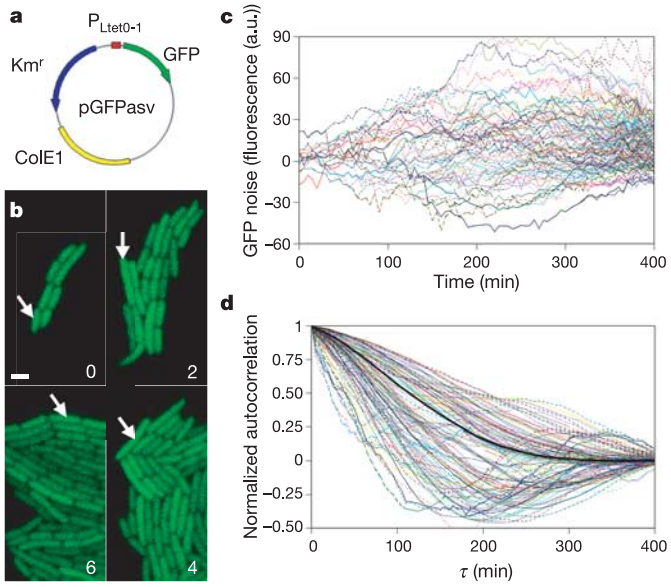


**Figure 1 | Measurement of noise frequency ranges using fluorescence time-lapse microscopy.** **a**, Plasmid pGFPasv containing the constitutively expressed GFP (110-min half-life) gene circuit. **b**, Bihourly (time in hours shown at the bottom right of images) snapshots of fluorescence in pGFPasv cell cultures (doubling time = 59 min; scale bar = 2 μm). The arrows follow one trajectory through six cell divisions. **c**, **d**, Noise in GFP concentration (**c**) and normalized autocorrelation functions (**d**) for all trajectories tracked from the experiment shown in **b**. The composite autocorrelation is shown as a bold black curve. Fluorescence in **c** is given in arbitrary units (a.u.).

[1]Molecular-Scale Engineering and Nanoscale Technologies Group, and [2]Computer Science and Mathematics Division, Oak Ridge National Laboratory, Bethel Valley Road, Oak Ridge, Tennessee 37831, USA. [3]University of Tennessee, Knoxville, Tennessee 37996, USA.

**Box 1 | Noise frequency range**

The noise frequency range is determined by the nature of the noise sources and gene circuit filtering. Fluctuations generated within the gene circuit (intrinsic noise) arise from the random timing and discrete nature of molecular transitions (for example, transcription, translation, decay or dilution through growth, and multimerization[9,10]). Extrinsic noise arises from the intrinsic noise of global sources (for example, fluctuations in ribosome or RNA polymerase populations) or of upstream genes in a regulatory cascade[7]. Intrinsic noise sources have wide frequency ranges, while extrinsic sources are confined to a lower-frequency range by their own gene circuit filtering[2].

The frequency range is found from the normalized autocorrelation function ($\Phi(\tau)$) of noise in a reporter protein concentration. Total noise in the protein concentration is produced by the sum of intrinsic and extrinsic noise source components filtered primarily by protein dilution through cell growth (rate $= \delta$) and protein decay (rate $= \gamma$) such that

$$\Phi(\tau) = W_E\left(\frac{\delta+\gamma}{\gamma}e^{-\delta\tau} - \frac{\delta}{\gamma}e^{-(\delta+\gamma)\tau}\right) + W_I e^{-(\delta+\gamma)\tau}$$

where $W_E$ and $W_I$ account for the relative contributions of extrinsic and intrinsic noise sources, and we have assumed that the frequency range of the extrinsic noise source is set by the cell growth rate[2].

We define the noise frequency range ($F_N$) as

$$F_N = \frac{1}{\tau_{1/2}}$$

where $\tau_{\frac{1}{2}}$ is the value of $\tau$ where $\Phi(\tau)$ drops to $\frac{1}{2}$. Slower fluctuations remain correlated over longer periods and therefore have lower values of $F_N$.

Theoretical analysis predicts that negative autoregulation increases the noise frequency range such that[11]:

$$F_{N\_autoreg} = (1+|T|)F_{N\_unreg}$$

$T$ is a unitless parameter proportional to the degree to which the autoregulated gene circuit resists changes in the equilibrium protein concentration (strength of regulation)[11]. The measured noise frequency range can be used to determine the strength of regulation using the equation above.

protein decay rate (Fig. 2b). Varying temperature changes the rates of all reactions, and while noise magnitude is sensitive to all of these changes, the noise frequency range of constitutively expressed circuits is mainly sensitive to protein dilution and decay rates only (see the Supplementary Information).

Significant variation from the noise frequency range predicted from decay and dilution rates indicates additional structure beyond the simple components of the constitutively expressed gene circuit. Most of the effects that have been considered (for example, extrinsic noise[1,2], protein–DNA binding in transcriptional control[12,16], protein dimerization[17], GFP maturation (see the Supplementary Information)) lower the noise frequency range. To test the predicted increased noise frequency range with negative autoregulation[11], we constructed circuits with the gene for the protein TetR inserted upstream of *gfp*, creating a transcriptional fusion (pTetR–GFPasv; Fig. 3a). This circuit was negatively autoregulated, as its expression was repressed by TetR binding to operator sites in the promoter[18]. A control circuit without autoregulation was also tested, in which a chromosomal copy of *tetR* was constitutively expressed from the $P_{N25}$ promoter. In both cases, repression was relieved by addition of anhydrotetracycline (ATc) to the growth medium, and thus allowed the modulation of GFP expression (Fig. 3b).

To determine if ATc had an effect on noise spectra independent of the autoregulation of the TetR circuit, we measured the noise frequency range of the pGFPasv circuits in media supplemented with 100 ng ml$^{-1}$ of ATc. There was a marked modification in the noise frequency range distribution (Fig. 3c), indicating a change in either the processing of the noise or the nature of the noise sources.

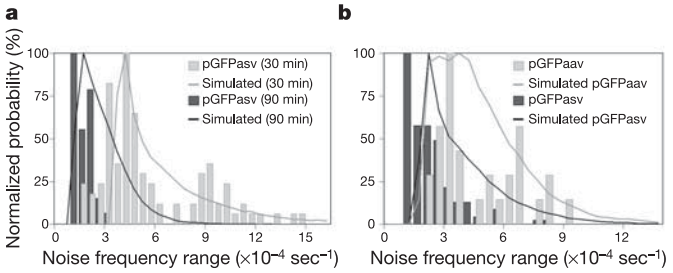


**Figure 2 | Effects of cell doubling time and protein half-life on noise frequency range.** Measured distributions are shown as vertical bars and simulated distributions as solid lines. **a**, Shift in noise frequency range for the pGFPasv circuit as doubling time increases from ~30 min (100 trajectories; T = 32 °C) to ~90 min (120 trajectories; T = 22 °C). **b**, Shift in noise frequency range as protein decay time decreases from 110 min (pGFPasv; 59-min doubling time; 154 trajectories; T = 26 °C) to 60 min (pGFPaav; 56-min doubling time; 33 trajectories; T = 26 °C).

Our modelling points to the latter, with ATc inhibition of translation leading to a whitening of extrinsic noise, which we then explored using a stochastic simulation model that included ribosome–ATc heterodimer formation (see the Supplementary Information). The frequency range distribution extracted from these simulations was compared to the measured distribution (Fig. 3c), with both showing a characteristic peak shift and peak broadening. Although not conclusive, this gross agreement between measured and simulated distributions supports the hypothesis that the mechanism of ATc-mediated noise frequency range modulation is an increase in high-frequency content of the global extrinsic noise associated with translation, and a reduction of the weighting of extrinsic noise.

We measured noise frequency range distributions of pTetR–GFPasv and the control cells grown in media with 100 ng ml$^{-1}$ of ATc. Composite noise frequency ranges of the negatively autoregulated pTetR–GFPasv exceeded those of the constitutively expressed pGFPasv in 100 ng ml$^{-1}$ of ATc by as much as ~2–3-fold (Figs 3d and 4a), whereas the control circuits showed no noise frequency range increase (Fig. 4a). The negative autoregulation-mediated noise remodelling was seen as an increase of the noise frequency range (Fig. 4a) and as a modification of the shape of the distribution (Fig. 3d and Supplementary Information). Autoregulation frequency response is limited by protein decay and dilution, and therefore has a larger effect on slower fluctuations than on faster fluctuations. Noise trajectories that would have clustered at the lower end of the frequency range distribution in unregulated cells are pushed to higher values by negative autoregulation, while those in the higher-frequency tail of the distribution are only weakly affected (Fig. 3e). This results in frequency range distributions closer to normal distributions (Fig. 3d). The frequency shift and the change in distribution shape are indicative of the presence of negative autoregulation.

The magnitude of the autoregulation-mediated frequency shift was indicative of the strength of regulation (Box 1), which varied significantly as a function of cell doubling time (Fig. 4a). The measurements indicate that regulation strength is small at both fast and slow rates of cell growth, with a peak at intermediate levels of cell growth. In our gene circuit model (Fig. 4b), regulation strength is the product of terms that describe (1) the change in free (not bound to ATc and capable of repression) TetR dimer concentration in response to changes in transcription rate, and (2) the change of transcription rate in response to changes in free TetR dimer binding to the operator (see the Supplementary Information). Our measurements consistently showed lower average fluorescence at high cell growth rates (data not shown), indicating that GFP (and probably TetR) concentration was reduced by rapid dilution. At high growth

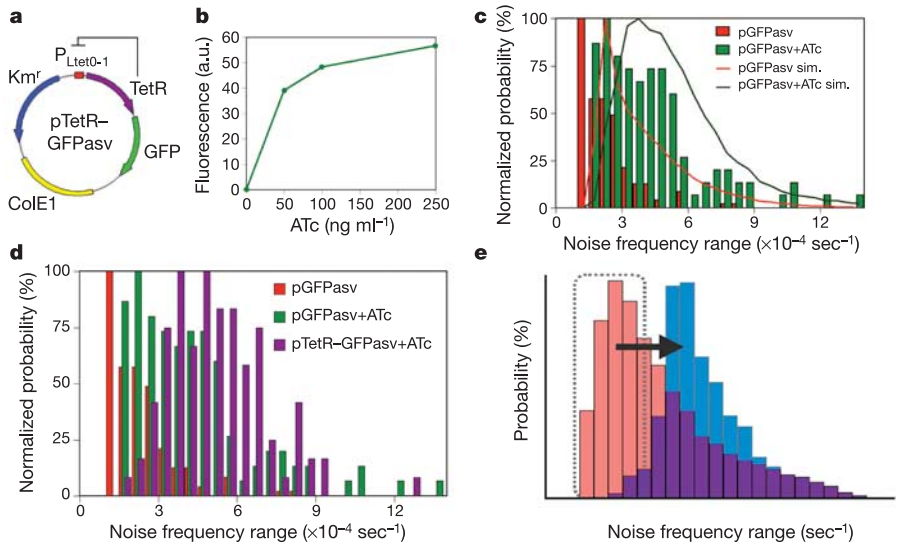


**Figure 3 | Effect of negative autoregulation on noise frequency range.** **a**, pTetR–GFPasv negatively autoregulated gene circuit with **b**, repression strength modulated by ATc. **c**, Effect of ATc on the noise frequency range of the unregulated pGFPasv circuit (doubling time ~60 min; 154 trajectories without ATc; 114 trajectories with ATc). sim., simulated. **d**, Negative autoregulation-mediated shift of noise frequency range (doubling time ~60 min; pGFPasv: 154 trajectories without ATc, 114 trajectories with ATc; pTetR–GFPasv: 114 trajectories). **e**, Model of the shift of frequency range distribution shape due to negative feedback. The red bars represent an unregulated circuit distribution; blue bars represent distribution for the circuit with negative autoregulation. The dashed box and arrow show the shift of the low-frequency trajectories to the centre of the distribution while the higher-frequency trajectories are unaffected. Fluorescence in **b** is given in arbitrary units (a.u.).

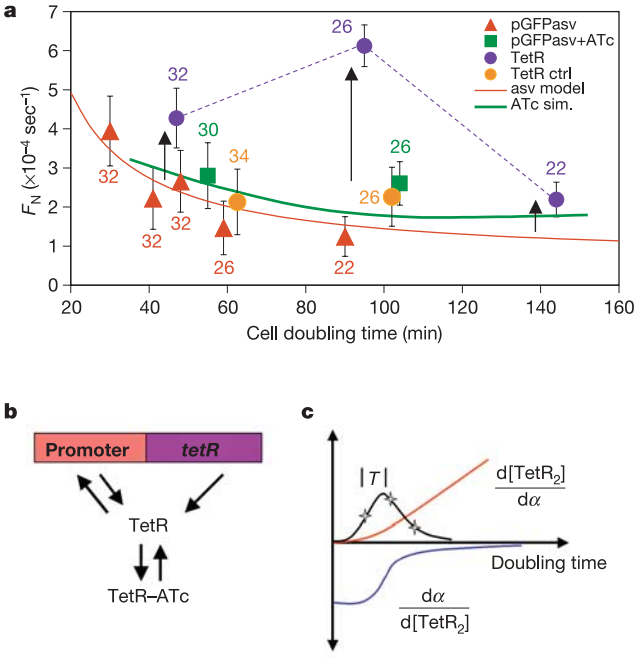


**Figure 4 | Regulation strength modulation of noise frequency range.** **a**, Noise frequency range versus doubling time. Measured points are shown with $\pm 1\sigma$ error bars estimated from simulation (see the Supplementary Information). The red line is the analytical curve (see Box 1 and the Supplementary Information) for the pGFPasv circuit, and was found from the analytical expression for the autocorrelation function (see Box 1). The green line is the simulated curve (see the Supplementary Information) for pGFPasv + 100 ng ml$^{-1}$ ATc and was found from the simulation of the pGFPasv circuit with ATc–ribosome binding (see the Supplementary Information). Vertical black arrows represent regulation strength determined by the shift of the noise frequency range. The temperature (in °C) of each experiment is indicated by each data point. The TetR data points are for the circuit with autoregulated *tetR* expression, while the TetR ctrl data points are for the circuit with constitutive *tetR* expression. **b**, **c**, Regulation of the pTetR–GFPasv circuit. The red curve shows the concentration of free TetR dimer ([$TetR_2$]) variation with transcription rate ($\alpha$); the blue curve shows transcription rate variation with [$TetR_2$]; and the black curve shows net regulation strength. The stars illustrate points on the regulation curve similar to the TetR data in **a**.

rates, repression strength was low as most TetR was bound with ATc. Conversely, at low cell growth rates, abundant free TetR dimer was formed, but regulation strength was low as the repression curve saturated[12,16]. The result was a regulation curve that peaked at intermediate cell growth rates where there was an adequate abundance of free TetR dimer, but not so much that the repression curve had saturated (Fig. 4c).

Previous work demonstrated the noise magnitude damping effect of negative autoregulation[19]. We have demonstrated that gene circuits also manipulate noise spectra, impacting the regulatory effect of the noise as it propagates through the gene network. We verified the link between gene circuit structure and the noise frequency range, and showed that changes in gene circuit parameters (for example, cell growth and protein decay rates) modulate the noise frequency range. Our results show a shift of noise spectra to higher frequencies and a remodelling of the noise frequency range distribution that is characteristic of negative autoregulation. This frequency shift may have biological relevance, as higher-frequency noise is more easily filtered out by downstream gene circuits in a regulatory cascade, and therefore has little regulatory impact[11]. Noise may play a beneficial role in some gene circuit functions[17,20,21], and circuit structure may have evolved to optimize rather than minimize noise. The theory described here predicts that positive regulation, which plays an important role in many gene circuit functions[17,22,23], increases noise magnitude while shifting noise frequency range downward into a more regulatory-relevant regime where it may play a role in the function of some genetic switching elements[17]. Intriguingly, the noise frequency range distributions provided a means for evaluating a hypothesis of the mechanism of ATc-mediated remodelling of noise spectra in unregulated gene circuits (see the Supplementary Information), suggesting that the coupling of spectral measurements and simulation provides a new tool for probing mechanistic details of gene circuit regulation.

## METHODS

**Synthetic gene circuits.** The high-copy plasmid pGFPasv (pZE21-GFPasv; ref. 24) was used both directly and as the platform for further genetic manipulation. This plasmid contains the *gfpmut3** reporter gene, modified to include a carboxy-terminal amino-acid tag previously shown to facilitate accelerated degradation of GFP protein within the cell[15], and is expressed from the strong promoter $P_{Ltet0-1}$ (ref. 18). GFP variants with alternative half-lives were created by replacement of the 3′ tag of the *gfp* gene with synthetic oligonucleotides using standard methods[15]. The *tetR* gene was amplified by polymerase chain reaction (PCR), cloned, sequenced and then subsequently digested and inserted upstream of *gfp-asv* to form the ATc-inducible, negatively autoregulated transcriptional fusion in plasmid pTetR–GFPasv. The

non-autoregulated control system was created by transforming the pGFPasv plasmid into *E. coli* DH5αPRO (BD Biosciences), which contains a chromosomal insertion of the *tetR* gene behind the $P_{N25}$ promoter.

**Cultures, growth conditions and imaging.** *E. coli* TOP10 (Invitrogen) cells were used for all experiments unless otherwise noted. For slide experiments, overnight cultures were grown at 28 °C in M9 medium supplemented with 100 mM leucine and 10% (v/v) Luria–Bertani broth, plus kanamycin ($50\,\mu g\,ml^{-1}$) and ATc (anhydrotetracycline; Acros) when appropriate. Cultures were transferred 1:3 into fresh media and allowed to recover for ~1 h before spreading 10 μl onto freshly prepared glass microscope slides coated with the same media containing 1% (w/v) Sea Plaque low-melt agarose (FMC). Coverslips were applied and the slides were allowed to incubate 1 h at 28 °C before imaging. Slides were imaged every 5 min using the Leica SP2 confocal system with an excitation wavelength of 488 nm and emission wavelength at 500–564 nm. Temperature was maintained using a heating lamp and monitored with a Hanna KJF thermocouple.

**Data processing.** Noise traces were extracted from the images for nearly all possible trajectories in each experiment. Custom Matlab (Mathworks) programs were used to find mean fluorescence of an entire cell population and to estimate population doubling time from an exponential growth curve. Normalized autocorrelations functions (ACFs) for individual trajectories ($\Phi_m$) were found from the noise time series ($X_m(nT_s)$) using a biased algorithm[25]

$$\Phi_m(jT_s) = \frac{\sum_{n=1}^{N-j} X_m(nT_s)X_m((n+j)T_s)}{\sum_{n=1}^{N} X_m^2(nT_s)}$$

where $T_s$ was the five-minute sampling interval, $n$ was the sample number (1, 2,…, $n$), and $j$ had integer values from 0 to $n-1$. The composite autocorrelation function ($\Phi_c$) for $M$ cell trajectories was found using:

$$\Phi_c(jT_s) = \frac{\sum_{m=1}^{M}\sum_{n=1}^{N-j} X_m(nT_s)X_m((n+j)T_s)}{\sum_{m=1}^{M}\sum_{n=1}^{N} X_m^2(nT_s)}$$

**Simulations.** Gillespie's stochastic simulation algorithm[13] was used to generate simulated estimates of ACFs, error bars, $F_N$ histograms, and $F_N$ behaviour as a function of doubling time. The models accounted for extrinsic and intrinsic noise sources, binding of 30S ribosomal subunits by ATc, appropriate temperature corrections, and protein sinks consisting of decay and dilution via stochastically timed cell division processes (see the Supplementary Information). Individual simulations were designed to closely match experimental conditions in terms of numbers of cells tracked, distribution of cell division frequencies, and experimental duration. Sets of many individual simulations were used to define mean system behaviour, its variability, and experimental uncertainty.

**Received 23 April; accepted 5 September 2005.**


1. Elowitz, M. B., Levine, A. J., Siggia, E. D. & Swain, P. S. Stochastic gene expression in a single cell. *Science* **297,** 1183–1186 (2002).
2. Rosenfeld, N., Young, J. W., Alon, U., Swain, P. S. & Elowitz, M. B. Gene regulation at the single-cell level. *Science* **307,** 1962–1965 (2005).
3. Swain, P. S., Elowitz, M. B. & Siggia, E. D. Intrinsic and extrinsic contributions to stochasticity in gene expression. *Proc. Natl Acad. Sci. USA* **99,** 12795–12800 (2002).
4. Blake, W. J., Kaern, M., Cantor, C. R. & Collins, J. J. Noise in eukaryotic gene expression. *Nature* **422,** 633–637 (2003).
5. Raser, J. M. & O'Shea, E. K. Control of stochasticity in eukaryotic gene expression. *Science* **304,** 1811–1814 (2004).
6. Ozbudak, E. M., Thattai, M., Kurtser, I., Grossman, A. D. & van Oudenaarden, A. Regulation of noise in the expression of a single gene. *Nature Genet.* **31,** 69–73 (2002).
7. Pedraza, J. M. & van Oudenaarden, A. Noise propagation in gene networks. *Science* **307,** 1965–1969 (2005).
8. Thattai, M. & van Oudenaarden, A. Intrinsic noise in gene regulatory networks. *Proc. Natl Acad. Sci. USA* **98,** 8614–8619 (2001).
9. Kaern, M., Elston, T. C., Blake, W. J. & Collins, J. J. Stochasticity in gene expression: From theories to phenotypes. *Nature Rev. Genet.* **6,** 451–464 (2005).
10. Rao, C. V., Wolf, D. M. & Arkin, A. P. Control, exploitation and tolerance of intracellular noise. *Nature* **420,** 231–237 (2002).
11. Simpson, M. L., Cox, C. D. & Sayler, G. S. Frequency domain analysis of noise in autoregulated gene circuits. *Proc. Natl Acad. Sci. USA* **100,** 4551–4556 (2003).
12. Simpson, M. L., Cox, C. D. & Sayler, G. S. Frequency domain chemical Langevin analysis of stochasticity in gene transcriptional regulation. *J. Theor. Biol.* **229,** 383–394 (2004).
13. Gillespie, D. T. Exact stochastic simulation of coupled chemical reactions. *J. Phys. Chem.* **81,** 2340–2361 (1977).
14. Gibson, M. A. & Bruck, J. Efficient exact stochastic simulation of chemical systems with many species and many channels. *J. Phys. Chem. A* **104,** 1876–1889 (2000).
15. Andersen, J. B. *et al.* New unstable variants of green fluorescent protein for studies of transient gene expression in bacteria. *Appl. Environ. Microbiol.* **64,** 2240–2246 (1998).
16. Kepler, T. B. & Elston, T. C. Stochasticity in transcriptional regulation: Origins, consequences, and mathematical representations. *Biophys. J.* **81,** 3116–3136 (2001).
17. Cox, C. D. *et al.* Analysis of noise in quorum sensing. *OMICS* **7,** 317–334 (2003).
18. Lutz, R. & Bujard, H. Independent and tight regulation of transcriptional units in *Escherichia coli* via the LacR/O, the TetR/O and AraC/$I_1$-$I_2$ regulatory elements. *Nucleic Acids Res.* **25,** 1203–1210 (1997).
19. Becskei, A. & Serrano, L. Engineering stability in gene networks by autoregulation. *Nature* **405,** 590–593 (2000).
20. Arkin, A., Ross, J. & McAdams, H. H. Stochastic kinetic analysis of developmental pathway bifurcation in phage lambda-infected *Escherichia coli* cells. *Genetics* **149,** 1633–1648 (1998).
21. Thattai, M. & van Oudenaarden, A. Stochastic gene expression in fluctuating environments. *Genetics* **167,** 523–530 (2004).
22. Becskei, A., Seraphin, B. & Serrano, L. Positive feedback in eukaryotic gene networks: cell differentiation by graded to binary response conversion. *EMBO J.* **20,** 2528–2535 (2001).
23. Isaacs, F. J., Hasty, J., Cantor, C. R. & Collins, J. J. Prediction and measurement of an autoregulatory genetic module. *Proc. Natl Acad. Sci. USA* **100,** 7714–7719 (2003).
24. Elowitz, M. B. & Leibler, S. A synthetic oscillatory network of transcriptional regulators. *Nature* **403,** 335–338 (2000).
25. Bendat, J. S. & Piersol, A. G. *Data: Analysis and Measurement Procedures* (Wiley, New York, 2000).


**Supplementary Information** is linked to the online version of the paper at www.nature.com/nature.

**Acknowledgements** We thank I. Golding and J. Dunlap for advice on sample preparation and imaging, and M. Elowitz, J. Collins and T. Gardner for the gift of plasmids. This work was supported by the National Academies Keck Futures Initiative, the DARPA Bio-Computation Program, the NSF, the DOE Office of Advanced Scientific Computing Research, and was a user project of the Oak Ridge National Laboratory (ORNL) Center for Nanophase Materials Sciences (CNMS). D.W.A. acknowledges support from an ORNL CNMS Research Scholar Fellowship. R.D.D. acknowledges support from the DOE Science Undergraduate Laboratory Internship program.

**Author Contributions** D.W.A., M.S.A., J.M.M., C.D.C. and M.L.S. planned the experimental, analytical and computational work. D.W.A., R.D.D., and J.R.W. performed the time-lapse microscopy measurements. M.S.A., J.R.W. and G.S.S. were responsible for the synthetic biology. D.W.A., R.D.D., C.D.C., J.M.M. and M.L.S. analysed the experimental data. J.M.M., N.F.S. and C.D.C. were responsible for simulations. C.D.C. and M.L.S. developed the frequency domain analytical approach. M.L.S. was responsible for integration of experimental, analytical and computational components.

**Author Information** Reprints and permissions information is available at npg.nature.com/reprintsandpermissions. The authors declare no competing financial interests. Correspondence and requests for materials should be addressed to M.L.S. (simpsonML1@ornl.gov).